Bone SPECT of the Spine: A Comparison of Attenuation Correction Techniques

James A. Case, Robert Licho, Michael A. King and John P. Weaver

Departments of Nuclear Medicine and Surgery, University of Massachusetts Medical Center, Worcester, Massachusetts

Image artifacts from variable self-attenuation are recognized as major sources of diagnostic uncertainty in SPECT. For myocardial perfusion studies, an attenuation map is often obtained from a separate transmission study. However, for many applications such as bone SPECT, it has been believed to be unnecessary to obtain a transmission study to correct for the effects of attenuation. We have had significant success in clinical management of lower spine pain using bone SPECT. This success has led us to consider SPECT for the management of cervical spine pain. Cervical spine reconstructions without attenuation correction are difficult to interpret, because the high attenuation in the mandible and skull tends to decrease estimates of activity of the upper cervical spine, and the lower cervical/upper thoracic vertebrae are obscured by the shoulders. We present a technique that uses downscatter to provide attenuation correction for these acquisitions and compare it with other recognized attenuation correction techniques. **Methods:** An emission study is acquired using two windows: one for obtaining the photopeak data and another for obtaining the downscattered photons. A body outline is estimated from these datasets using a projection data thresholding method. From this outline, a uniform attenuation map is created using attenuation coefficients appropriate for ^{99m}Tc in water (0.154 cm^{-1}). These maps are used in SPECT reconstruction using ordered-subset expectation maximization (OSEM). This method is compared with (a) no attenuation correction (NC), (b) conventional Chang attenuation correction based on the interactive determination of the body outline from the ^{99m}Tc emission photopeak data (ChangAC) and (c) OSEM correction using attenuation maps estimated with a line source and fanbeam collimators (transAC). **Results:** Patient studies using scatterAC demonstrated a significant improvement in the uniformity of estimated cervical spine uptake in normal patients, compared with either NC or ChangAC. Results using scatterAC were similar to those of transAC. We also observed significant improvement in uniformity using scatterAC in SPECT of the lower back in obese patients, as well as the relative limitations of scatterAC versus nonuniform, transmission-based attenuation correction. **Conclusion:** Comparisons with reconstructions using transmission data for estimating attenuation demonstrate that reasonable quantitative accuracy can be obtained in SPECT of the cervical spine using this simple attenuation estimate. Both scatterAC and transAC appear to provide consistent and expected uniform spine uptake in the cervical spines of normal patients.

Received Mar. 4, 1998; revision accepted Sep. 22, 1998.

For correspondence or reprints contact: Robert Licho, MD, Department of Nuclear Medicine, University of Massachusetts Medical Center, 55 Lake Ave. North, Worcester, MA 01655.

Key Words: bone SPECT; spine; attenuation; back pain

J Nucl Med 1999; 40:604–613

Image artifacts from variable self-attenuation are recognized as major sources of diagnostic uncertainty in SPECT (*1–3*). The best known errors from this type of artifact have been described in SPECT myocardial imaging, in which attenuation from the diaphragm, breast and anterior chest wall have been shown to cause apparent, but erroneous, image defects. Attenuation artifacts have been described in other areas of SPECT such as brain imaging; however, these have not been shown to produce critical errors in interpretation such as those in myocardial imaging.

Several articles have described the usefulness of bone SPECT in the management of back pain. With few exceptions (*4,5*), these have been limited to SPECT of the lower back (*6,7*). To date, few studies have prospectively evaluated the clinical effectiveness of bone SPECT (*8*). However, several groups have presented the use of SPECT in directing back pain management (*9–11*). We have used bone SPECT successfully in the clinical management of lower back pain since the introduction of multidetector SPECT imaging in our department in 1991. SPECT images have complemented structural imaging studies, often providing a single active focus when structural studies reveal multiple, possibly in part chronic, non–pain-producing abnormalities or no abnormalities at all. We have used abnormal uptake on SPECT studies to help guide facet and intradisk injections of steroid/lidocaine, as well as surgery such as diskectomy and fusion. Initial response from the anesthetic component of steroid/lidocaine injections has also provided accuracy data on the use of SPECT, as well as structural imaging in back pain management (*11*).

When attempting SPECT of the cervical spine, however, we have encountered a systematic apparent increase in counts in the cervical spine. We have noted this in patients referred for evaluation of neck symptoms and subsequently in history- and symptom-free controls. Uniform, ^{99m}Tc photopeak edge-detection-based attenuation correction has produced variable results in changing this pattern. This has hampered our ability to detect and exclude focal abnormalities in the spine, as well as to differentiate diffuse abnormal

uptake from increased uptake as a result of less attenuation at the level of the midcervical spine relative to the level of the skull and thoracic spine. These difficulties have prompted us to evaluate the extent of attenuation artifact and the effectiveness of different methods for obtaining attenuation estimates and correction in this group of patients.

Many methods, of varying rigor, have been proposed to correct for attenuation artifact, all of which use either a measurement or estimate of attenuation to correct the SPECT dataset (*12*). The most accurate method currently available to correct for attenuation is an attenuation "map" using an external transmission source. Transmission imaging produces a patient-specific dataset (i.e., correct for individual body shape and content of differing attenuators such as bone, muscle and air spaces), which can be used for attenuation correction of a patient emission study. The attenuation dataset can be acquired simultaneously with the emission study or sequentially. It contributes an insignificant (<1%) additional radiation dose. However, transmission-based attenuation correction requires that the camera be physically modified with hardware to mount and control external radiation sources. This can be expensive and is not commercially available on all SPECT systems.

Because of the rigorous hardware and software of the transmission source-based methods, quicker and simpler methods have been attempted for use in estimating attenuation maps. One such approach is to approximate the body outline of the patient and then apply a constant attenuation coefficient within the interior of the outline to form patient-specific attenuation maps. Several methods can approximate the body outline. One of the earliest methods was orthogonal images from paired point sources to which ellipsoids were fit and placed on opposite sides of the patient (*13*). A more recent method has been the determination of the edges of the patient from photopeak or Compton scatter window projection images with reconstruction of the outlines from these edges (*14–17*). Other methods use direct estimation of the outlines from photopeak or Compton scatter window reconstructed slices (*18–21*). All of these segmentation methods are limited by the ability of the clinical tracer to produce a body outline and by the use of a uniform estimate of attenuation rather than a measurement of the true, nonuniform attenuation within that body. However, if the relative importance of measurement of nonuniform attenuation resulting from bone, soft tissue and lungs is minor compared to accurate body outline measurement, then significant attenuation correction might be obtained without a direct measurement of patient-specific attenuation (e.g., transmission imaging).

We have applied a method for estimating the body outline using projection data from a combination of the photopeak window and a Compton scatter window. The Compton scatter window is used because the scatter photons will illuminate the edges of the patient even though the skeleton has nearly completely taken up the pharmaceutical. The body outline is determined from the sum of the photopeak and scatter window projections by using an automated background determination. This method for determining the body outline from the projection data is more sensitive to the location of the patient boundary because of improved contrast of the object-to-background in the projection images. Attenuation correction is then applied to the image by reconstructing the emission data with the ordered-subset expectation maximization (OSEM) iterative reconstruction technique and these uniform attenuation estimates (*22,23*). This method was compared with OSEM of the emission data corrected using a transmission attenuation measurement as well as with uncorrected and photopeak-based uniform correction.

MATERIALS AND METHODS

Projection-Based Determination of Body Outline

Two methods of improving the sensitivity of the edge detection algorithm to the object boundary were applied: projection data-based reconstruction algorithm and the addition of a second energy window for scattered radiation (*23*). A projection-based edge-detection algorithm was chosen because of the higher contrast between the object and background relative to reconstruction based algorithms. To further improve the contrast between the patient and the background a second, simultaneous lower energy window of the scattered radiation was acquired. The scattered and photopeak radiation were combined into a single body outline estimate. At each projection angle, a background threshold was used to determine which pixels imaged the patient and which did not. By excluding all pixels outside the patient at all angles, a convex body contour was determined. Figure 1 illustrates this three-dimensional body contour in a healthy man.

For attenuation correction of the cervical spine, a uniform attenuation coefficient of $\mu = 0.15\ cm^{-1}$ was assigned to all of the detector bins within the boundary. The emission data were reconstructed with three iterations of the OSEM algorithm (*22*), which divided the data into 12 subsets. Reconstruction time for 64 slices using 128 × 128 pixel sampling was 25 min. Because the boundary was determined automatically and all slices in the field of view were reconstructed, the reconstruction program was run without user interaction.

Reconstruction-Based Edge Detection Method

The body contour method described in the previous section was compared with a reconstruction-based, segmentation algorithm. The attenuation correction method applied was the uniform attenuation correction method used on the Picker Odyssey system (Picker International, Cleveland, OH). This method uses a four-point (left lateral, right lateral, anterior and posterior) ellipsoid to define the body contour. These four points are determined automatically from a filtered backprojection (FBP) reconstruction of the photopeak data and can subsequently be modified manually. A uniform attenuation map is assigned inside the body contour and a zero-order Chang correction is applied to the FBP reconstruction of the data (*24*).

Fanbeam Transmission Tomography and Attenuation Estimate

Nonuniform estimates of the attenuation map were made using fanbeam transmission tomography (*25*). On a triple-head SPECT system, the transmission system consists of a fanbeam converging

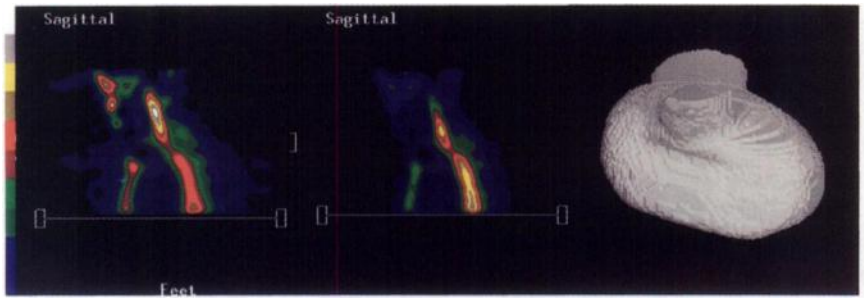

FIGURE 1. (Left) Sagittal view of nonattenuation-corrected (NC) SPECT in healthy, compact, muscular 50-y-old man. (Right) Three-dimensional body contour generated from scatter and photopeak projection data. (Center) Same sagittal slice using scatter/photopeak attenuation estimate and OSEM.

collimator on one of the camera heads and a line source of activity at the focal line of the fanbeam collimator. A set of projections through the object is taken and from those projections a three-dimensional reconstruction of the attenuation is made. The strengths of this system include (a) the attenuation map is patient specific, (b) the values obtained for the attenuation coefficients are close to the "good geometry" values due to the inherently low scatter fraction in transmission SPECT imaging, (c) a single line source is easy to mount and shield and (d) by having the line source at the focal line of the fanbeam collimator, no scanning motion is required as is necessary with some parallel-hole collimator systems (*26*). This system is limited when applied to attenuation correction of the cervical spine, because the patient, specifically the shoulders, may not be entirely in the field of view for all projections. This truncation leads to a fully sampled inner region and a poorly sampled outer region in the attenuation estimate. In the reconstruction of the attenuation map, the poor sampling in the outer region leads to very large distortions in the attenuation estimate outside the fully sampled region. We correct for the truncation in the transmission data by using the uniform attenuation map determined from the projection-based body outline method and applying a spatially varying gamma prior (*23*). This is applied only to the data outside the fully sampled region. The gamma prior method was used because it preserves the total line integrals of attenuation along each line of sight and restores much of the detail of the attenuation estimate in the outer, truncated regions.

Data Acquisitions

Data were acquired on a Prism 3000 triple-head camera system (Picker International), equipped with the Simultaneous Transmission-Emission Protocol (STEP) attenuation correction package. The standard clinical dose of 20 mCi ^{99m}Tc-methylene diphosphonate was administered intravenously 2–3 h before imaging. Two low-energy, ultra-high-resolution parallel collimators were placed on two of the camera heads and a 65-cm fanbeam collimator was placed on the camera head opposite the transmission source. Emission and transmission data were acquired simultaneously. The transmission source was a 60-mCi line source of ^{153}Gd (100 keV photopeak). For the emission data, two energy windows were acquired; one for the photopeak of ^{99m}Tc (140% ± 7.5% keV) and a large Compton downscatter window (108% ± 15% keV). For the transmission data, a single energy window was acquired at 100% ± 7.5% keV. Data was stored in a 128 × 128 matrix and a 0.317-cm pixel size. SPECT acquisition was performed using 3.75° steps in step-and-shoot acquisition mode using 15 s per stop.

Data Reconstruction and Attenuation Correction

Data were compared using four different reconstruction protocols: (a) non–attenuation-corrected FBP (NC), (b) uniform attenuation correction using FBP of the photopeak data and reconstruction-based Chang attenuation correction (ChangAC), (c) uniform attenuation correction using the projection/scatter-based, OSEM iterative algorithm (scatterAC) and (d) nonuniform attenuation correction using truncation-corrected transmission data and the OSEM iterative reconstruction algorithm (transAC). The NC and ChangAC data were reconstructed using filtered backprojection and a ramp filter. ScatterAC and transAC were reconstructed using an attenuated radon transform projector model in the OSEM algorithm, in which three iterations and 12 subsets of the OSEM algorithm were used. All reconstruction data were postfiltered with a three-dimensional parametric Weiner filter and subsequently rendered in three orthogonal (transverse, sagittal and coronal) projections.

Patients

Subjects for the study were patients who volunteered to have SPECT acquisition of the spine using the STEP system. Normal subjects were selected from this group as those patients undergoing bone scans who had no history of arthritis or of cervical spine injury or pain. Such patients might typically have a lower extremity complaint as their indication for bone scanning. Because of the possibility of differing extents of attenuation error in patients of different morphologies and variable results of the different correction techniques depending on these morphologies, as well as to sample the effect of the different correction techniques in a patient with an a priori, likely focal bone SPECT abnormality, five patients underwent quantitative analysis. Patients 1 and 2 were two normal average-sized and -shaped males; patient 3 was a large (mesomorphic) male with a clinical, radiographic and mild planar scintigraphic abnormality in the cervical region; patient 4 was a normal, average-sized and -shaped female; and patient 5 was a normal, petite and thin (i.e., ectomorphic) female. A cervical SPECT of an additional normal, compact and muscular male is also illustrated (Fig. 1), as is a lumbar SPECT of a moderately obese (endomor-

phic) male and a normal male patient demonstrating nonuniform attenuation effects in the thorax.

Data Analysis

Reconstructions were analyzed qualitatively to assess detection and quantitatively to measure the effect of attenuation correction. Display and quantitation of the images was performed on data normalized to the highest pixel in the spine (in the field of view). Quantitative analysis of the reconstruction was done by analyzing 5 small regions of interest (ROIs) in the upper cervical (UC), midcervical (MC), lower cervical (LC) and upper thoracic (UT) territories, for a total of 20 ROIs in each patient. The average counts within the ROIs were determined, and the SD between ROIs was calculated. As a measure of the degree of attenuation artifact, we compared the ratio of the MC (least attenuation) to the UT (greatest attenuation) for each of the correction techniques (Table 1). The transmission-based attenuation-correction method (transAC) was used as our gold standard for comparing the spine count distribution using NC, scatterAC and ChangAC. Theoretically, therefore, an MC/UT greater than that obtained from transAC would be an undercorrection (or, in the case of NC, a noncorrection); an MC/UT less than that of transAC would be an overcorrection.

RESULTS

In the first average-size normal male subject, we observed considerable variation in uniformity of spinal uptake depending on the method of correction. There was an overestimation of activity in the upper and MC spine using NC, as seen in Figures 2A and 3. As a result, the MC/UT in the NC reconstruction (i.e., without attenuation correction) was 1.39 ± 0.10. In contrast, the MC/UT was 0.99 ± 0.08 using scatterAC and 1.01 ± 0.10 using the gold standard transAC. The ChangAC method, with an MC/UT of 0.43 ± 0.05, underestimated the relative amount of neck attenuation. The reconstruction-based body outline detection algorithm of ChangAC failed to locate the patient edge. The photopeak edge detection method instead localized to the outer boundary of the cervical vertebrae. These differing estimates begin to illustrate the significant impact of attenuation and accurate attenuation correction.

TABLE 1
Ratios of Midcervical to Upper Thoracic ROIs in Five Patients

	NC	ChangAC	ScatterAC	TransAC
Normal male	1.39 ± 0.10	0.43 ± 0.05	0.99 ± 0.08	1.01 ± 0.10
Normal male II	1.39 ± 0.22	0.89 ± 0.24	0.79 ± 0.22	0.88 ± 0.17
Large male	1.69 ± 0.05	0.49 ± 0.08	1.19 ± 0.09	1.12 ± 0.06
Normal female	1.41 ± 0.12	0.44 ± 0.04	1.10 ± 0.09	0.93 ± 0.14
Small female	1.01 ± 0.06	0.48 ± 0.04	0.96 ± 0.04	0.95 ± 0.03

NC = nonattenuation-corrected filtered backprojection; ChangAC = uniform attenuation correction using Chang method; ScatterAC = uniform attenuation correction using projection scatter-based OSEM iterative algorithm; TransAC = nonuniform attenuation correction using truncation-corrected transmission data and the OSEM iterative reconstruction algorithm.

In a second normal and average-size male (Fig. 2B), the scatterAC method performed similarly to ChangAC and transAC in estimating spinal counts: MC/UT (NC) = 1.34 ± 0.22, MC/UT (scatterAC) = 0.79 ± 0.22, MC/UT (transAC) = 0.88 ± 0.17 and MC/UT (ChangAC) = 0.89 ± 0.24). In this example, the ChangAC method performed comparably to transAC and better than in the previous patient, because it successfully determined the patient outline from the reconstructed data. This illustrates how the failure in accuracy of ChangAC in the previous patient example can be attributed more likely to poor boundary determination than to the mathematically approximate nature of the ChangAC algorithm applied to the FBP dataset. NC still markedly overestimated the MC/UT compared with transAC.

In sagittal slices from the clinical and radiographic lower cervical lesion of the large mesomorphic male (Fig. 2C), the effect of tissue attenuation was quite dramatic, with an MC/UT of 1.69 ± 0.05 for NC. The conventional ChangAC method produced an equally dramatic underestimation of cervical spine counts, with an MC/UT of 0.49 ± 0.08. There was a significant improvement in the uniformity of spinal counts when the scatterAC method was applied (MC/UT = 1.19 ± 0.09, compared with 1.12 ± 0.06 for transAC). In sagittal slices that correspond radiographically and clinically to the patient's cervical lesion (Fig. 4A), there was a focal region of increased tracer uptake on scatterAC and transAC. This focus was not seen using the NC method. Using the ChangAC method, there was considerable variability in the cervical count profile, depending on the edge detection threshold used. The best ChangAC profile that could be generated is the example shown in Figure 4A, and it demonstrated mildly excess lesion counts relative to the MC spine when compared to the gold standard transAC. Nevertheless, in this particular patient, an acceptable profile was possible.

A normal and average-size female (Fig. 2D) was also studied. In this patient, the MC/UT was 1.41 ± 0.12, 1.10 ± 0.09, 0.93 ± 0.14 and 0.44 ± 0.04, using NC, scatterAC, transAC and ChangAC, respectively. These results were comparable to those seen in the normal males.

In the normal small (petite-thin) female patient (Figs. 2E and 4B), we observed a relatively small impact of tissue attenuation on the SPECT reconstruction. The MC/UT was 1.01 ± 0.06 using NC, 0.96 ± 0.04 using the scatterAC method and 0.95 ± 0.03 using transAC. In small individuals, the effect of attenuation appears to be considerably less, as evidenced by the minor difference between NC and transAC. However, it is worth noting that the MC/UT was 0.48 ± 0.04 with the ChangAC method. Again, this was the result of the failure of the boundary detection algorithm to successfully locate patient edges. In instances such as these,

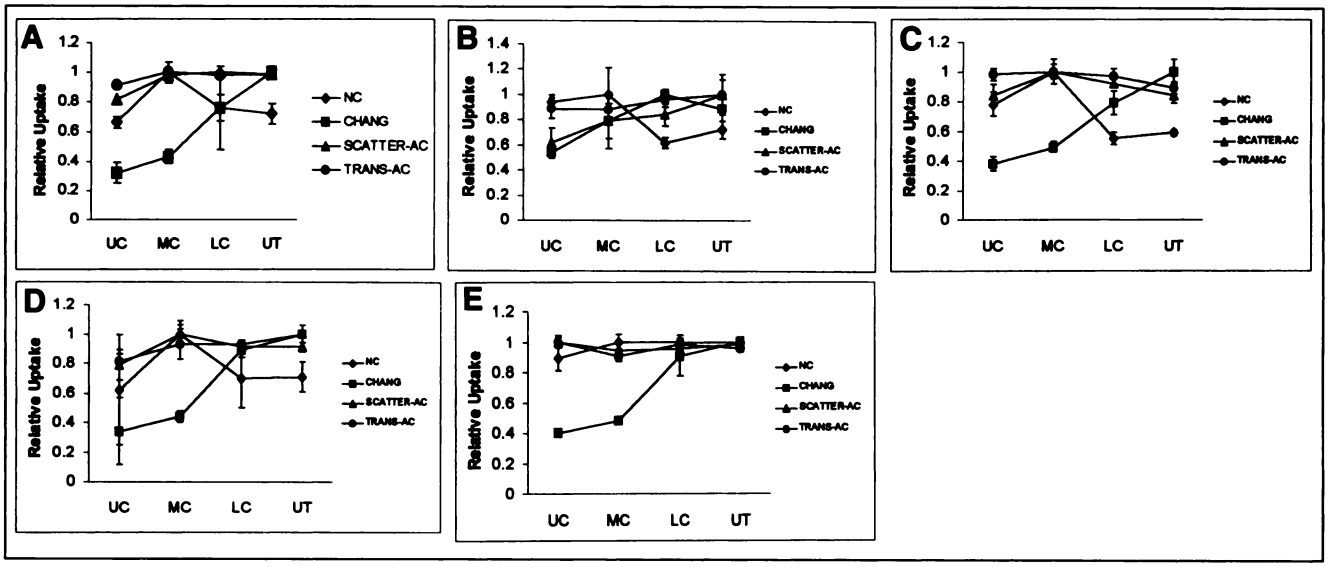

FIGURE 2. ROIs were measured in upper cervical (UC), midcervical (MC), lower cervical (LC) and upper thoracic (UT) territories, using each correction method. Average counts within ROIs were plotted normalized to highest count ROI per each method. Plots of four methods are presented in (A) normal male I, (B) normal male II, (C) large mesomorphic male with lower cervical clinical, radiographic and mild planar scintigraphic abnormality, but off the plane of the abnormality, (D) normal female I and (E) normal (petite-thin) female II. NC = no correction.

when Chang/photopeak edge detection inadvertently detects the vertebra rather than the soft tissue patient boundary, interactive boundary selection would partially improve the result. However, given the number of transverse slices that would need to be interactively drawn, this technique would greatly increase processing time and would still be limited to ellipsoid axial estimates.

Overall, these comparisons demonstrate that attenuation correction using an attenuation map determined from scatter-based projection data provided a reasonable compensation

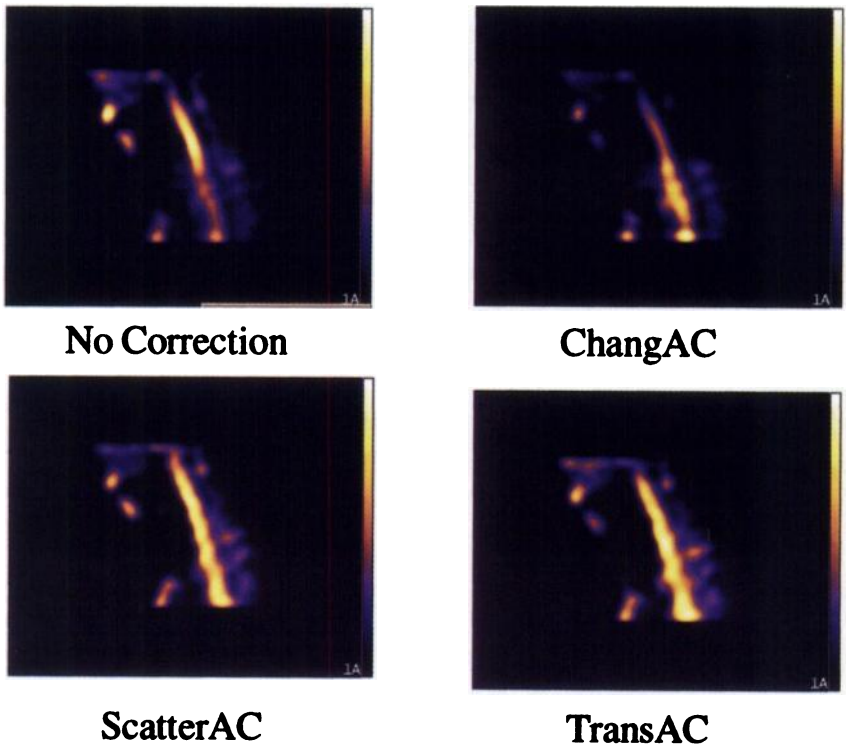

FIGURE 3. Images of normal average-size male illustrate overestimation of cervical spine using FBP with no attenuation correction (NC), underestimation using FBP with ChangAC and near-identical spinal uniformity using both scatterAC and transAC.

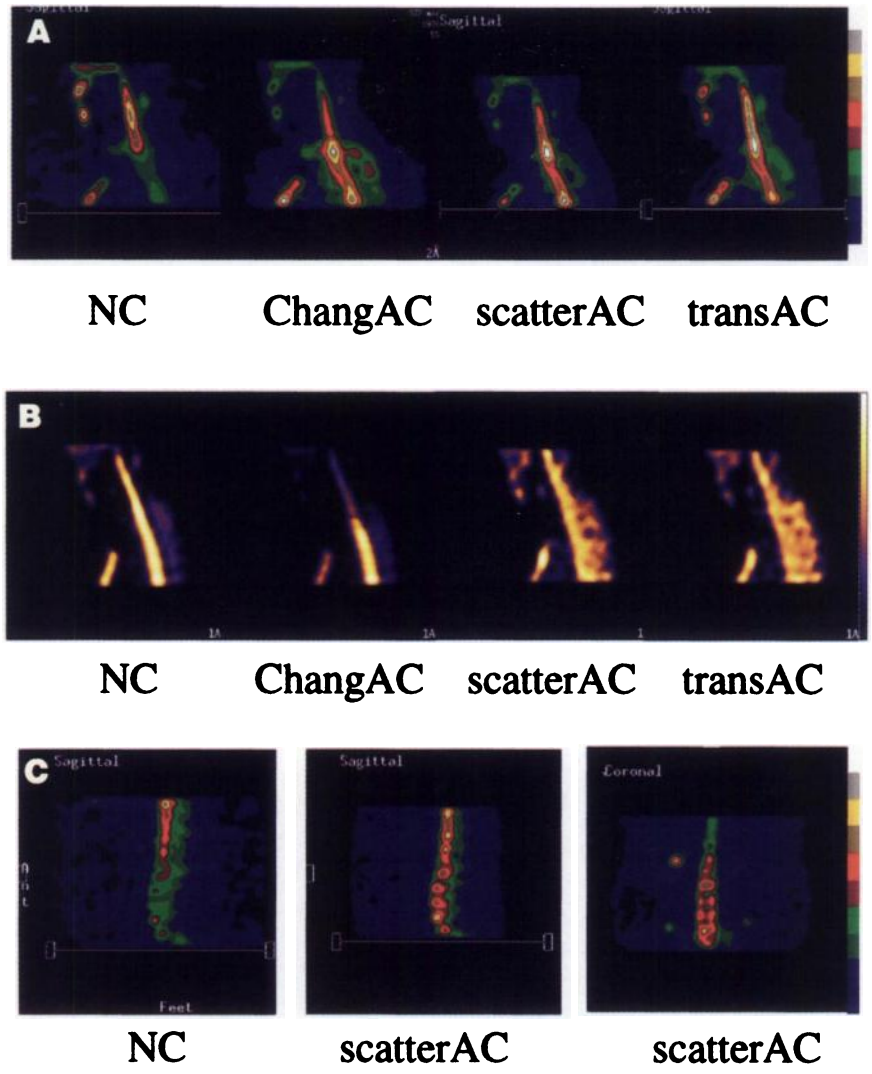

FIGURE 4. (A) Projections of large mesomorphic male from Figure 2C on plane of lower cervical abnormality, using NC, ChangAC, scatterAC and transAC. (B) Comparable sagittal projections using NC, ChangAC, scatterAC and transAC in normal petite-thin female. (C) Lumbar SPECT of obese male: sagittal NC (left), same sagittal slice using scatterAC (center) and coronal scatterAC (right).

for the variable attenuation between the head, neck and shoulder region in cervical spine studies. The impact of attenuation appears to be proportional to patient bulk or heft. The patient's sex did not appear to influence the results of the four techniques tested.

A thoracolumbar SPECT of a normal patient (Fig. 5) illustrates a phenomenon we have noted consistently when performing SPECT of this region. We consistently note a sharp gradient of activity in the transition of the lumbar to the thoracic spine, at the level corresponding to the diaphragm. This is a nonuniform attenuation effect caused by less attenuation by the lung soft tissue (approximately 1/3 the density of muscle and abdominal soft tissue) versus more attenuation by the abdominal (water density) tissue. This will result in uniformly higher thoracic vertebral counts with any method, including NC, scatterAC or ChangAC, which assumes a single uniform density within the patient boundary, and is only correctable using nonuniform attenuation correction (i.e., transAC). In the absence of large-field-of-view transAC capability, we cannot demonstrate the transAC method for correction of attenuation in this region.

A lumbar SPECT of an obese patient is presented, however, in which uniform correction using only a boundary determination appears to improve image quality significantly. Figure 4C demonstrates how the NC method results in a count-poor region of spine uptake corresponding to the region of greatest girth. ScatterAC detects this greater girth and adds counts at those levels, resulting in a dramatic recovery of uniformity throughout the lumbar spine in this otherwise normal patient.

DISCUSSION

Clinical use of bone SPECT in the management of patients with cervical spine problems has until now been limited by the variable attenuation present in the head, neck

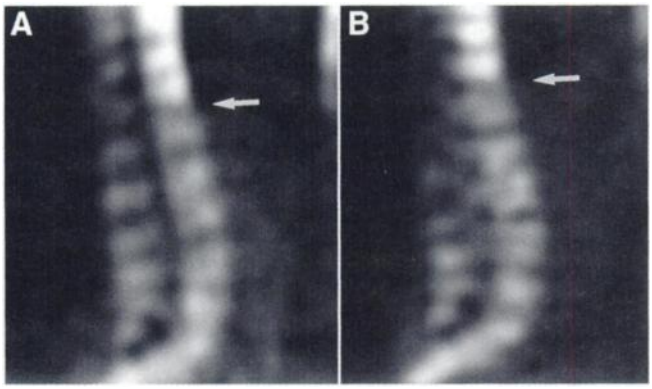

FIGURE 5. Comparable sagittal thoracolumbar views of normal male using NC (A) and scatterAC (B). Arrows denote level of diaphragm. Note marked increased spine estimate in transverse axes containing lung tissue (less true attenuation, therefore overestimated by NC, and not corrected by uniform [scatter] AC).

and shoulder regions. This variable attenuation complicates interpretation of spinal images by greatly reducing the number of counts received from the upper cervical and thoracic regions relative to the neck region. To date, clinical bone SPECT imaging has used either no attenuation correction or Chang correction using a uniform attenuation coefficient within the ^{99m}Tc photopeak boundary. We demonstrate how uncorrected images produce a dramatic and artifactual increase in cervical spine activity relative to counts attenuated by the shoulders and skull.

In addition, we show how ChangAC frequently, but unpredictably, underestimates the true relative counts of the cervical spine. The ideal bone scan contains minimal soft-tissue activity; however, this lack of soft-tissue counts results in poor statistics and contrast at the patient boundary. If the patient soft-tissue boundary is poorly identified, a deeper boundary is detected, usually outlining the neck vertebrae, skull and humeral heads. Such a boundary reasonably estimates skull/shoulder/thoracic attenuation but underestimates neck attenuation, resulting in erroneously low counts in the neck. This artifact, for example, can obscure an abnormal focus of high activity in the neck, producing a "pseudonormal" distribution instead of multifocal abnormal high activity, or can lead to a misdiagnosis of abnormally high activity in the undercorrected neck compared to the thoracic or high cervical spine (i.e., skull) region.

Use of TransAC as Gold Standard

We chose to use transmission-based attenuation correction as the gold standard for the true spine count distribution. The extent to which transmission-based attenuation correction approaches "truth" has been addressed and validated previously (*12,25*), using phantom data (scans of models containing known count concentrations, attenuation coefficients, locations and volumes). We examined these techniques in vivo and provided relative quantification (MC/UT) as an initial measure of the extent of difference between these methods. We did not attempt to formally validate transmission-based AC in vivo, although localization by visual inspection of orthogonal slices of attenuators, such as the mandible and shoulders, was used to attempt to predict expected sites of attenuation artifact and successful correction. We postulated a priori, on the basis of vertebral size, function and weight bearing, that normal cervical vertebrae would be from mildly less to equal in counts ($\leq$10%) compared to thoracic vertebrae and that there would be no abrupt change in counts between any adjacent normal vertebrae. Based on these nonabsolute methods, we found no instance in our analyzed patients where we suspected transAC to be substantively different from "truth."

Need for Attenuation Correction in Bone SPECT and Unreliability of Reconstruction-Based Boundary Detection Algorithms

Both nonattenuation corrected images (NC) and ^{99m}Tc-photopeak edge detection-based uniform attenuation correction (ChangAC) tended to dramatically over- and underestimate cervical spine counts, respectively, typically by 30%–50%. On lower spine studies, this is the typical percentage increase of a focal SPECT abnormality relative to homologous regions when ROI analysis is used, and thus is of enough magnitude to interfere with accurate scan interpretation. NC predictably overestimated cervical counts, apparently in proportion to patient mass or weight. However, ChangAC, as measured by MC/UT, was unpredictable from subject to subject. This instability was due to inconsistency of the method in correctly locating the patient boundary. Manual override of boundary selection in ChangAC was of limited benefit, because of the limitation of such boundary estimates to slice-by-slice sequences of ellipses and of very limited visualization of soft tissue, particularly in the neck. ChangAC was the most time-costly method, thus in multiple manual reprocessing attempts and thus delays in scan interpretation. Figure 6 compares attenuation maps obtained from transmission and scatter data with body outline estimates using ChangAC in the same patient. The Chang method (Fig. 6a) was applied, unsuccessfully, to detect the transition from mandible (top of image) to the trapezius muscles, producing an asymmetric ROI including an area clearly outside (anterior and to the right of) the patient. One slice lower, where the shoulder joints were now more evident, a symmetric ROI resulted (Fig. 6b). A change in the edge detection threshold of a single increment, however, resulted in a dramatically larger ellipse (Fig. 6c), with a difference in the spine count estimate in this region of more than 20%.

ScatterAC

We found scatterAC to range from reasonably accurate (i.e., 90% of transAC) to indistinguishable from transAC. We have also found this method to be more stable and predictable than NC and ChangAC, but to yield occasional focal errors relative to transAC. The use of combined projection data from a photopeak window and a Compton scatter window for estimating the body outline was more sensitive in locating the patient boundary because of im-

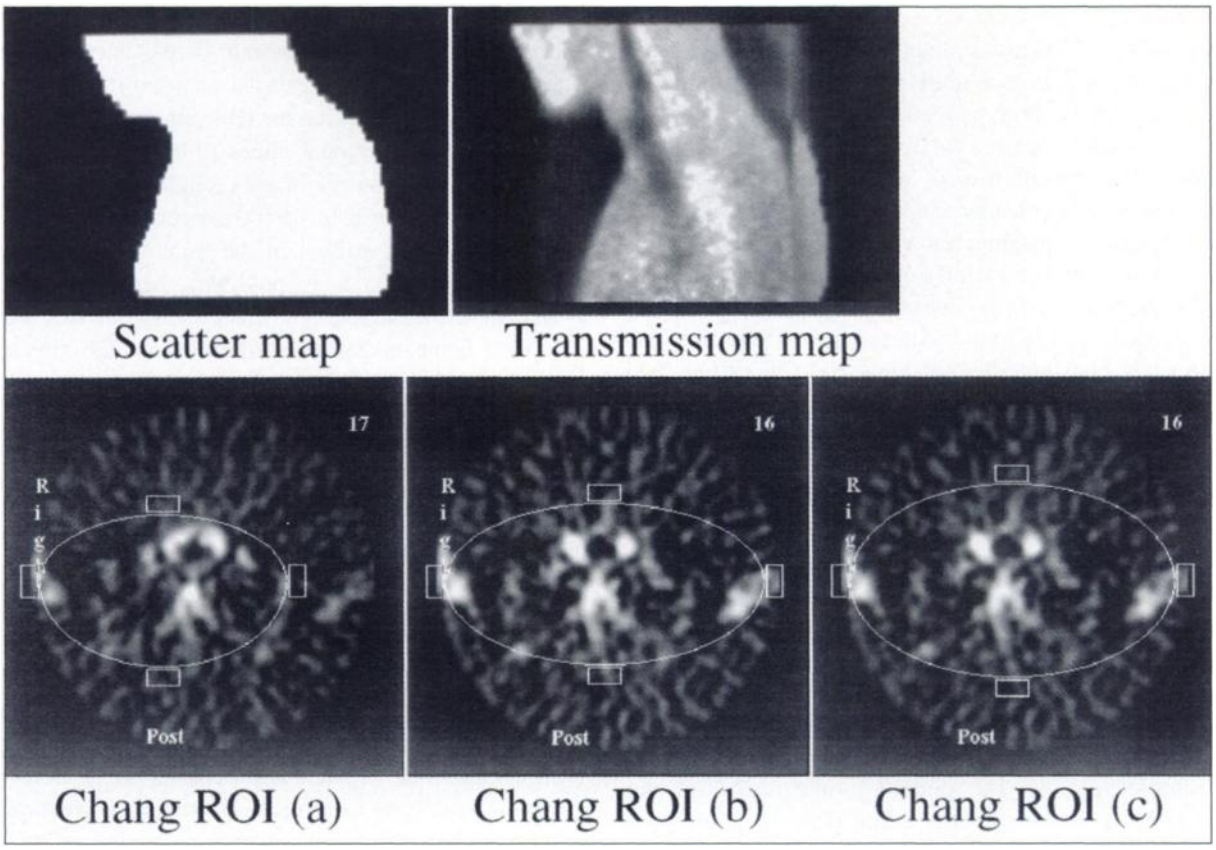

FIGURE 6. (Top) Sagittal images of transmission and scatter-based attenuation maps. Note detection of air in the oropharynx and trachea, as well as imaging table in transmission map, and near identical outline, including table, using scatter map. Evident in ROI with use of ChangAC on emission dataset of same patient are difficulty in detecting the symmetric transition from mandible to trapezius muscles and also inclusion in ROI of area clearly outside (anterior and to right of) patient. One slice lower, now with shoulder joints in better view, images (b) and (c) show difference in ROI produced by change of one increment in edge detection threshold. This change produced difference in spine count estimate in this region of more than 20%.

proved contrast of the object-to-background in the projection images. Comparison with transAC demonstrated that attenuation correction using a projection-based detected boundary with a single attenuation coefficient within that boundary (i.e., uniform correction) provided a reasonable compensation for the variable attenuation between the head, neck and shoulder region in cervical spine studies. This suggests that the more important factor determining patient attenuation in these cervical SPECT studies is the accurate estimate of the patient boundary, with variable attenuation within that boundary being less important.

Fundamental Limitations of ScatterAC

We found scatterAC to be infrequently and mildly limited in its ability to contour the patient boundary when soft-tissue scatter counts were very low in abundance. In addition, scatterAC has a limited ability to contour the radical concavities that may be encountered in the transition from mandible to neck. Finally, the assumption of a uniform attenuation coefficient can result in inaccuracy when imaging a region in which true attenuation is clearly nonuniform. For example, we illustrate how, in regions of dramatic transition in soft-tissue density (and therefore the attenuation coefficient), such as above and below the diaphragm, the assumption of uniform attenuation leads to an inaccurate relative spine count estimate. This problem may occur wherever a uniform attenuation estimate is used for attenuation correction of regions obscured by large, differing attenuators, and therefore affects scatterAC, ChangAC and NC equally. As stated earlier, we did not find this to be a critical phenomenon at the level of the cervical spine or apices of the lungs, probably because of the relatively limited area or volume of the lung apices, humeral heads and mandibular bone, relative to the cross-sectional area differences between the shoulders, neck and skull.

Hardware-Related Limitations

Transmission-based attenuation correction using a converging system such as our fanbeam/opposing line source assumes certain spatial constraints. The line source must remain at the focal line of the fanbeam collimator, which occasionally does not allow a sufficient range of imaging radii. Our system would not allow complete camera rotation around very obese patients, because of the proximity of the line source and holder. In large patients around whom camera rotation was possible, there was still a large acquisition radius that, because of collimator convergence, resulted in increased image truncation. This limitation was much

more significant in the transAC method (as a result of its use of converging collimators), but can influence even the scatterAC technique (which needs only parallel-hole collimators) in sufficiently large patients. The truncation problem can be obviated by use of a larger-field-of-view detector. Therefore, for clinical use, a large-field-of-view system ordinarily would be considered optimal for scatterAC imaging and transAC imaging, as well as on systems with scanning line source transmission hardware. Because we wanted to provide a side-by-side comparison of transAC and scatterAC and did not have scanning line source transAC capability on our large-field-of-view SPECT system, we were limited to our smaller-field-of-view system. Between nonuniform but truncated transAC and uniform large-field-of-view scatterAC, relative inaccuracy may depend on patient size and can be determined only from quantitative comparison with a nontruncated transAC acquisition. After our method of compensation for truncation was applied, we could not find visual evidence of a truncation artifact in the spine regions of our analyzed patients, but still considered truncation a potential problem worthy of further analysis.

Figure 7 illustrates a transmission map of a recent bone SPECT in which there is significant truncation of data and resultant error in estimating the attenuation map outside the fully sampled region. The outline in the region of the imaging table is larger than the actual table and, similarly, the facial outline is overestimated. Note that positioning of this patient was such that the thoracic spine was near or outside the fully sampled region (when the detector is lateral to the patient), which resulted in erroneous localization behind the patient of the attenuation from the spine. Such an overestimation of attenuation in the slices containing these overestimations of body outline would greatly increase the count estimate in those slices (and thus decrease the relative count estimate in the remaining slices, in this case the midcervical spine). The distorted anatomy and visual evidence of error in estimating the table attenuation coefficient, as depicted on orthogonal slices of the attenuation map, served as quality-control images, analogous to a rotating cine or sinogram used to detect patient motion. (Note the minimal truncation artifact in the transAC and scatterAC maps in Figure 6). It is possible, then, to experience significant, error-producing artifact using transAC, particularly with fanbeam collimation. However, the attenuation map, which can be rendered orthogonally, permits a systematic review for evaluating the accuracy of the attenuation estimation. The most appropriate solution to this potentially critical problem of image truncation is to perform bone SPECT with transAC using a large rather than small-field-of-view SPECT system and a transmission geometry that avoids truncation altogether.

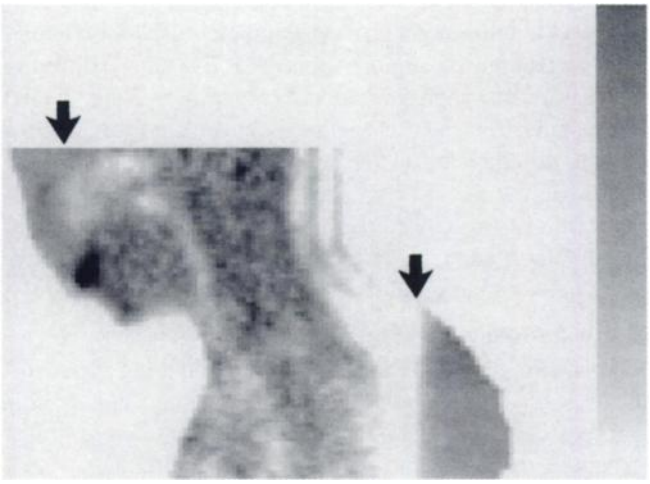

FIGURE 7. Sagittal reconstruction of transmission map of patient illustrates error resulting from truncation using small-field-of-view SPECT system and low count transmission source. Note overestimation of body and table contour (peripheral to arrows) that would result in over-replacement of spine counts in respective axial slices. Arrows also mark transition from fully sampled region (inside arrows) to non-fully sampled region (peripheral to arrows).

CONCLUSION

In our experience with bone SPECT of the cervical spine, we have been limited by tremendous imaging inaccuracy when using either no attenuation correction or reconstruction photopeak-based uniform attenuation correction. We have found that accurate attenuation correction, using either scatterAC or transAC, has made bone SPECT of the cervical spine possible where previously it was not. In our experience with transAC or scatterAC in cardiac, brain and bone SPECT, we have found its application in bone SPECT to be the most significant and, indeed, compulsory when imaging the cervical spine. The scatterAC method can be applied to iterative reconstruction, obviating the need for user interaction and, because no transmission map is needed, may be especially advantageous on systems that do not offer transmission-based attenuation correction, such as present single-detector SPECT cameras, or in situations of hardware, software or other clinical or logistical conflict with transmission AC. ScatterAC may thus be a very useful software component on all SPECT systems, even when these include transAC hardware and software. ScatterAC may be of limited value when the assumption of uniform attenuation within the body outline is wrong, such as in the transition from above to below the diaphragm. When available and not limited by truncation, transAC is probably the optimal attenuation correction method for clinical use, as it appears to provide both consistent and uniform spine uptake as is expected in normal patients. When using projection-based attenuation correction (transAC or scatterAC), one must remain alert to truncation error (especially when the patient extends beyond the axial, fully sampled field of view of the system). Orthogonal reconstructions of the attenuation map can be rendered using the projection-based AC methods. These attenuation maps may be useful clinically in that their routine inspection can help to avoid misleading artifacts.

ACKNOWLEDGMENTS

Supported in part by U.S. Public Health grant HL50394. The contents are solely the responsibility of the authors and do not necessarily represent the views of the U.S. Public Health Service. We also thank Dr. Stephen Glick for his help in preparing illustrations.

REFERENCES

1. Datz FL, Gullberg GT, Zeng GL, et al. Application of convergent-beam collimation and simultaneous transmission emission tomography to cardiac single-photon emission computed tomography. *Semin Nucl Med.* 1994;24:17–37.
2. Depuey EG, Garcia EV. Optimal specificity of thallium-201 SPECT through recognition of imaging artifacts. *J Nucl Med.* 1989;30:441–449.
3. Ficaro EP, Fessler JA, Shreve PD, Kritzman JN, Rose PA, Corbett JR. Simultaneous transmission/emission myocardial perfusion tomography. *Circulation.* 1996;93:463–473.
4. Seitz JP, Unguez CE, Corbus HF, Wooten WW. SPECT of the cervical spine in the evaluation of neck pain after trauma. *Clin Nucl Med.* 1995;20:667–673.
5. Prekeges JL, Eisenberg B, Price-Eng K. Effective SPECT of the cervical spine. *J Nucl Med Technol.* 1996;24:100–103.
6. Gates GF. SPECT imaging of the lumbosacral spine and pelvis. *Clin Nucl Med.* 1988;13:907–914.
7. Collier BD, Kir KM, Mills BJ, et al. Bone scan: a useful test for evaluating patients with low back pain. *Skeletal Radiol.* 1990;19:267–270.
8. Littenberg B, Siegel A, Tosteson ANA, Mead T. Clinical efficacy of SPECT bone imaging for low back pain. *J Nucl Med.* 1995;36:1707–1713.
9. Laubenbacher C, Wicke-Wittenius S, Boning G, Krapf M, Langhammer HR. High resolution bone SPECT of the lumbar spine for localization of active arthrosis of facet joints [abstract]. *J Nucl Med.* 1995;36:26.
10. Ryan PJ, Fogelman I. SPECT bone scanning can predict successful facet joint injection [abstract]. *J Nucl Med.* 1995;36:26.
11. Licho R, Soares E, Feinbloom D, Weaver J. Comparison of bone SPECT with structural imaging modalities in directing the management of back pain [abstract]. *J Nucl Med.* 1997;38:29.
12. King MA, Tsui BMW, Pan T-S. Attenuation compensation for cardiac single-photon emission computed tomographic imaging: Part 1. Impact of attenuation and methods of estimating attenuation maps. *J Nucl Cardiol.* 1995;2:513–524.
13. Larsson S A. Gamma camera emission tomography. *Acta Radiol.* 1980;363(suppl): 38–39.
14. Hosoba M, Wani H, Toyama H, Murata H, Tanaka E. Automated body contour detection in SPECT: effects on quantitative studies. *J Nucl Med.* 1986;27:1184–1191.
15. Picker International, Nuclear Medicine Division. *Odyssey Software Reference.* Document 960474. Cleveland, OH: Picker International; 1996:A4–10.
16. Tomitani T. An edge detection algorithm for attenuation correction in emission CT. *IEEE Trans Nucl Sci.* 1987;34:309–312.
17. Macey DJ, DeNardo GL, DeNardo SJ. Comparison of three boundary detection methods for SPECT using Compton scattered photons. *J Nucl Med.* 1988;29:203–207.
18. Hebert TJ, Gopal SS, Murphy P. A fully automated optimization algorithm for determining the 3-D patient contour from photo-peak projection data in SPECT. *IEEE Trans Med Imaging.* 1995;14:122–131.
19. Bergstrom M, Litton J, Eriksson L, Bohn C, Blomqvist G. Determination of object contour from projections for attenuation correction in cranial positron emission tomography. *J Comp Assist Tomogr.* 1982;6:363–372.
20. Minato K, Tang Y-N, Bennett GW, Brill AB. Automatic contour detection using a fixed-point Hachimura-Kuwahara filter for SPECT attenuation correction. *IEEE Trans Med Imaging.* 1987;6:126–133.
21. Pan T-S, King MA, Penney BC, Rajeevan N, Luo D-S, Case JA. Reduction of truncation artifacts in fan beam transmission by using parallel beam emission data. *IEEE Trans Nucl Sci.* 1995;42:1310–1320.
22. Hudson MH, Larkin RS. Accelerated image reconstruction using ordered subsets of projection data. *IEEE Trans Med Imaging.* 1994;13:601–609.
23. Case JA, Pan T-S, King MA, Luo D-S, Penney BC. Reduction of truncation artifacts in fan-beam transmission imaging using a spatially varying Gamma prior. *IEEE Trans Nucl Sci.* 1995;42:2260–2265.
24. Chang W. A method of attenuation correction in radionuclide computed tomography. *IEEE Trans Nucl Sci.* 1978;25:638–643.
25. Tung CH, Gullberg GT, Zeng GL, Christian PE, Datz FL, Morgan HT. Non-uniform attenuation correction using simultaneous transmission and emission converging tomography. *IEEE Trans Nucl Sci.* 1992;39:1134–1143.
26. Tan P, Bailey DL, Meikle SR, Eberl S, Fulton RR, Hutton BF. A scanning line source for simultaneous emission and transmission measurements in SPECT. *J Nucl Med.* 1993;34:1752–1760.